

Accepted for publication in *The Astrophysical Journal*

Predictions of the High-Energy Emission from BL Lac objects: The Case of W Comae

M. Böttcher¹²

*Department of Physics and Astronomy, Rice University, MS 108,
6100 S. Man Street, Houston, TX 77005 - 1892, USA*

mboett@spacsun.rice.edu

and

R. Mukherjee

*Department of Physics and Astronomy, Barnard College and Columbia University, New
York, NY 10027, USA*

muk@astro.columbia.edu

and

A. Reimer

*Institut für Theoretische Physik IV, Ruhr-Universität Bochum, D - 44780 Bochum,
Germany*

afm@tp4.ruhr-uni-bochum.de

ABSTRACT

Spectral fitting of the radio through hard X-ray emission of BL Lac objects has previously been used to predict their level of high-energy (GeV – TeV) emission. In this paper, we point out that such spectral fitting can have very large uncertainties with respect to predictions of the VHE emission, in particular if no reliable, contemporaneous measurement of the GeV flux is available and the νF_ν peak (flux and frequency) of the synchrotron component is not very precisely known. This is demonstrated with the example of the radio-selected BL Lac object W Comae, which is currently on the source list of the STACEE and CELESTE experiments, based on extrapolations of the EGRET flux measured from

this source, and on model predictions from hadronic blazar jet models. We show that the best currently available contemporaneous optical – X-ray spectrum of W Comae, which shows clear evidence for the onset of the high-energy emission component beyond ~ 4 keV and thus provides a very accurate guideline for the level of hard X-ray SSC emission in the framework of leptonic jet models, still allows for a large range of possible parameters, resulting in drastically different > 40 GeV fluxes. We find that all acceptable leptonic-model fits to the optical – X-ray emission of W Comae predict a cut-off of the high-energy emission around ~ 100 GeV. We suggest that detailed measurements and analysis of the soft X-ray variability of W Comae may be used to break the degeneracy in the choice of possible fit parameters, and thus allow a more reliable prediction of the VHE emission from this object. Using the available soft X-ray variability measured by *BeppoSAX*, we predict a > 40 GeV flux from W Comae of $\sim (0.4 - 1) \times 10^{-10}$ photons $\text{cm}^{-2} \text{s}^{-1}$ with no significant emission at $E \gtrsim 100$ GeV for a leptonic jet model. We compare our results concerning leptonic jet models with detailed predictions of the hadronic Synchrotron-Proton Blazar model. This hadronic model predicts > 40 GeV fluxes very similar to those found for the leptonic models, but results in > 100 GeV emission which should be clearly detectable with future high-sensitivity instruments like VERITAS. Thus, we suggest this object as a promising target for VHE γ -ray and co-ordinated broadband observations to distinguish between leptonic and hadronic jet models for blazars.

Subject headings: galaxies: active — gamma-rays: theory — BL Lacertae objects: individual (W Comae)

1. Introduction

After the detection of 6 high-frequency peaked BL Lac objects (HBLs) with ground-based air Čerenkov telescope facilities, the field of extragalactic GeV – TeV astronomy is currently one of the most rapidly expanding research areas in astrophysics. The steadily improving flux sensitivities of the new generation of air Čerenkov telescope arrays (Konopelko 1999; Weekes et al. 2002) and their decreasing energy thresholds, provides a growing potential

¹Chandra Fellow

²Current address: Department of Physics and Astronomy, Clippinger 339, Ohio University, Athens, OH 45701, USA

to extend their extragalactic-source list towards intermediate and even low-frequency peaked BL Lac objects (LBLs) with lower νF_ν peak frequencies in their broadband spectral energy distributions (SEDs). Detection of such objects at energies $\sim 40 - 100$ GeV might provide an opportunity to probe the intrinsic high-energy cutoff of their SEDs since at those energies, $\gamma\gamma$ absorption due to the intergalactic infrared background is still expected to be negligible at redshifts of $z \lesssim 0.2$ (de Jager & Stecker 2002).

Theoretical predictions of the high-energy emission of BL Lac objects on the basis of their emission at lower frequencies (Stecker et al. 1996; Costamante & Ghisellini 2002) are essential for careful planning of future observations by ground-based VHE γ -ray observatories. Such studies have generally been restricted to considerations of the observed broadband spectral properties of potential candidate sources and have mostly been based on non-simultaneous spectral measurements alone. In this paper, we point out that such considerations can have very large uncertainties and ambiguities with respect to the predicted VHE emission. The importance and potential scientific return of including detailed variability information in the modeling of HBLs has been pointed out by Coppi & Aharonian (1999) who have shown the wide variety of correlated X-ray and VHE γ -ray variability patterns which can result in time-dependent synchrotron-self-Compton models for blazars. In particular, they have pointed out that combined X-ray spectral and variability information may be sufficient to predict the level of intrinsic TeV emission in HBLs, even if no direct measurements at GeV – TeV energies are available. Here, we will demonstrate that similar conclusions hold for LBLs, and investigate the example of the radio-selected BL Lac object W Comae (= ON 231 = 1219+285; $z = 0.102$), which is currently on the source list of the STACEE and CELESTE experiments. Its GeV – TeV source candidacy is based on the fact that W Comae has been detected by the EGRET instrument on board the *Compton Gamma-Ray Observatory* at energies above 100 MeV, exhibiting a very hard spectrum (von Montigny et al. 1995; Sreekumar et al. 1996). A power-law extrapolation of the average EGRET 0.1 – 10 GeV flux into the multi-GeV – TeV range yields a VHE flux well above the current detection threshold of both STACEE and CELESTE (see Fig. 3). Dingus & Bertsch (2001) also report on the detection of a 27.3 GeV photon from this source by EGRET in April 1993. Furthermore, Mannheim (1996) has predicted a TeV flux near the detection limit of the Whipple air Čerenkov telescope at the time, based on a proton-blazar model fit to a non-simultaneous broadband spectrum of W Comae.

The source was observed in a multiwavelength campaign in February 1996, covering the electromagnetic spectrum from GHz radio frequencies to TeV energies (Maisack et al. 1997). No TeV emission was detected by either Whipple or HEGRA.

While W Comae is generally observed to exhibit a typical one-sided jet morphology

in VLBI images, Massaro et al. (2001) report the detection of a weak apparent counter-jet component in 1999.13, if the brightest jet component with the flattest radio spectrum is identified with the core. Such a feature has not been found in any previous or later radio maps of the source. Massaro et al. (2001) demonstrate that it is implausible that this component is actually the emission from the counter-jet. Alternatively, they suggest, e.g., that it could be due to a small-angle displacement of the jet direction in a general configuration in which the jet is directed at a very small average angle with respect to the line of sight.

The most detailed currently available simultaneous broadband spectrum of W Comae has been measured in May 1998 (Tagliaferri et al. 2000) and is shown in Figs. 3 and 4. The X-ray spectrum has been measured by *BeppoSAX* and shows clear evidence for the intersection of the low-frequency (synchrotron) component and the high-frequency (Compton) component of the SED of W Comae at ~ 4 keV. There was clear evidence for variability on a ~ 10 hr time scale in the LECS count rate at photon energies of $0.1 - 4$ keV, while no evidence for variability was found in the MECS count rate at $4 - 10$ keV and the PDS count rate at $12 - 100$ keV. A 3σ upper limit of 40 % on the short-term variability amplitude in the MECS count rate could be derived in the May 1998 observations (Tagliaferri et al. 2000). The 4 individual spectral points in the EGRET energy range have been measured in March 1998, and are not strictly simultaneous to the *BeppoSAX* observations. The EGRET detection was at low significance (2.7σ), and allowed only a rather crude source localization to within 1.5° . We have calculated the spectrum of the source using 4 broad energy bins, as described more fully in §2.

The remainder of this paper is organized as follows: The re-analysis of the available EGRET data is presented in §2. In §3 we describe the leptonic jet model which we use to reproduce the broadband spectrum of W Comae. The modeling results and the model-dependent predictions for VHE emission from W Comae will be presented in §4. In §5 we discuss, how a detailed measurement and analysis of the photon-energy dependent fast X-ray variability of W Comae and other BL Lac objects might be used to break the degeneracy of model parameters still present in the pure spectral modeling using a leptonic jet model. A comparison to the modeling results and predictions of a hadronic jet model are presented in §6. We summarize in §7.

2. Gamma-Ray Observations

ON 231 is the suggested identification of the EGRET source 3EG J1222+2841, and the association of the EGRET source with this BL Lac object is based on probabilistic arguments. 3EG J1222+2841 was a weak EGRET source that was never detected at $> 6\sigma$

in any individual viewing period (VPs). The locations of low-confidence EGRET sources are not well-determined owing to the wide point spread function (PSF) at photon energies > 100 MeV (Thompson et al. 1993; Mattox, Hartman, & Reimer 2001), and identification of EGRET sources with counterparts based on position alone is difficult. Analysis of EGRET data from 1991 – 1995 yielded a 7.7σ detection and a hard spectrum with photon index $\alpha = 1.73 \pm 0.18$ (Hartman et al. 1999), and 3EG J1222+2841 was identified with ON 231 with “high confidence”. However, this identification was based on the $E > 1$ GeV position of Lamb & Macomb (1997) rather than the $E > 100$ MeV position, as is standard practice for EGRET sources.

Mattox, Hartman, & Reimer (2001) have recently done a quantitative re-evaluation of potential radio identifications for the 3EG radio sources by calculating the probability of each identification. They note that based on its $E > 100$ MeV position, 3EG J1222+2841 cannot be included in their list of high confidence identifications. Using the $E > 1$ GeV position, Mattox, Hartman, & Reimer (2001) get the probability of identification to be 4 %, which is classified as “plausible”. Future observations with GLAST will be important in determining the source position with more accuracy, and securing a more confident identification. For the purpose of our analysis, we assume that W Comae is the counterpart of 3EG J1222+2841. However, the low significance of the $\sim 2.7 \sigma$ detection in May 1998 and its non-simultaneity to the BeppoSAX observations prevents us from deriving any strong constraints from the EGRET flux or spectrum.

EGRET has observed 3EG J1222+2841 = W Comae several times since its launch in 1991. Table 1 lists the VPs during which the source was observed, and the corresponding integral fluxes for energies greater than 100 MeV. Only photons with inclination angles less than 30° were used for the analysis. For Phase 1 through Cycle 4 of the EGRET observations (1991 – 1995), Table 1 lists data from the 3EG catalog (Hartman et al. 1999). Three additional observations were made in Cycles 5, 7 and 9. We have analyzed these data using the standard EGRET data processing technique, as described in Mattox et al. (1996) and Hartman et al. (1999), and included them in the table. The light curve for 3EG J1222+2841 is shown in Fig. 1. The figure shows fluxes for all detections at a level greater than 2σ ; for detections below 2σ , upper limits at the 95 % confidence level are shown.

We have computed the background-subtracted γ -ray spectra of 3EG J1222+2841 for the strongest detections, as well as for March 1998, close to the time of the *BeppoSAX* observations. The spectra were determined by dividing the EGRET energy band of 30 MeV – 10 GeV into 4 bins, and estimating the number of source photons in each interval, following the standard EGRET spectral analysis technique (Nolan et al. 1993). We have fitted a single power law of the form $F(E) = k (E/E_0)^{-\alpha}$ photons $\text{cm}^{-2} \text{s}^{-1} \text{MeV}^{-1}$ to

the data, where $F(E)$ is the flux, E is the energy, α is the photon spectral index. Table 1 includes the photon spectral indices for the source in the four VPs. Figures 3 and 4 show both the average EGRET spectrum (1991 – 1995) from the 3rd EGRET catalog (Hartman et al. 1999) — as dot-dashed bow-tie outline —, as well as the spectrum measured in March 1998.

In addition to the EGRET observations, W Comae was observed by Whipple in March – April 1993 and March 1994. The source was not detected, and 3σ upper limits of 2.3×10^{-11} photons $\text{cm}^{-2} \text{s}^{-1}$ and 1.4×10^{-11} photons $\text{cm}^{-2} \text{s}^{-1}$, respectively, at $E > 0.3$ TeV were reported (Kerrick et al. 1995) for those two observing periods. Recently, the source has been of interest to the STACEE (Ong et al. 2001) and CELESTE (Smith 2002) experiments, operating in the energy range 50 – 250 GeV. Figures 3 and 4 show the sensitivities of the two experiments. STACEE observed W Comae in 1998 with a prototype experiment, and reported a preliminary 2σ (95 % confidence) upper limit of 2.4×10^{-10} photons $\text{cm}^{-2} \text{s}^{-1}$ (Theoret 2000), based on ~ 5 hr of data. Since these results are preliminary, we have not included them in the spectral fits shown in the figures.

3. Spectral modeling of W Comae using leptonic models

For the purpose of spectral modeling using a generic leptonic jet model, it is assumed that a population of ultrarelativistic, non-thermal electrons and positrons is injected instantaneously into a spherical emitting volume of co-moving radius R_b . The injected pair population is specified through a co-moving density n_e , low and high energy cutoffs γ_1 and γ_2 , respectively, and a spectral index p so that $n_e(\gamma) = K\gamma^{-p}$ for $\gamma_1 \leq \gamma \leq \gamma_2$ at the time of injection. The location of the injection site is characterized by its height z_i above the plane of a central accretion disk for which we have assumed a bolometric luminosity of $L_D = 10^{45}$ ergs s^{-1} . A magnetic field B_0 at the point of injection is chosen in equipartition with the nonthermal pair distribution at the time of injection, and decreases as $B = B_0 (z/z_i)^{-1}$. The emitting region moves with relativistic speed $v/c = \beta_\Gamma = \sqrt{1 - 1/\Gamma^2}$ along the jet which is directed at a small angle ($\theta_{\text{obs}} = 1^\circ$) with respect to the line of sight. The choice of a very small observing angle implies that the observer is located within the beaming cone of relativistically beamed emission from the emitting region for all values of Γ considered here, and is consistent with the moderate superluminal motion of $\beta_{\text{app}} \lesssim 2$ and the Massaro et al. (2001) result concerning the occasional two-sidedness of the radio structure observed in W comae, as mentioned in §1. The Doppler boosting of emission from the co-moving to the observer’s frame is determined by the Doppler factor $D = [\Gamma (1 - \beta \cos \theta_{\text{obs}})]^{-1}$.

Using the time-dependent radiation transfer code of Böttcher et al. (1997) and Böttcher

& Bloom (2000), we follow the evolution of the electron population and the radiation spectra as the emission region moves outward along the jet. Radiation mechanisms included in our simulations are synchrotron emission, Compton upscattering of synchrotron photons (SSC = Synchrotron Self Compton scattering: Marscher & Gear (1985); Maraschi, Celotti, & Ghisellini (1992); Bloom & Marscher (1996)), and Compton upscattering of external photons (EC = External Compton scattering), including photons coming directly from the disk (Melia & Königl 1989; Dermer, Schlickeiser, & Mastichiadis 1992; Dermer & Schlickeiser 1993), as well as re-processed photons from the broad line region (Sikora, Begelman, & Rees 1994; Blandford & Levinson 1995; Dermer, Sturmer, & Schlickeiser 1997). The broad line region is modelled as a spherical shell between $r_{\text{BLR,in}} = 0.2$ pc and $r_{\text{BLR,out}} = 0.25$ pc, and a radial Thomson depth $\tau_{\text{T,BLR}}$ which is considered a free parameter.

The most rapid variability has been observed in soft X-rays, where approximately symmetric flare profiles on a time scale of ~ 10 hr have been seen (Tagliaferri et al. 2000). This constrains the size of the emission region to be $R_b \lesssim D \times 10^{15}$ cm. For typical Doppler factors of $D \sim 10$, this motivates our choice of $R_b = 10^{16}$ cm, which we adopt throughout this paper.

The assumption that the magnetic field is in approximate equipartition with the emitting electron/positron population allows an independent estimate of the co-moving magnetic field: A power-law population of electrons with spectral index p , emitting a synchrotron νF_ν peak flux of $\nu F_\nu^{\text{pk}} = 10^{-10} f_{-10}$ ergs $\text{cm}^{-2} \text{s}^{-1}$ at a dimensionless photon energy $\epsilon_{\text{pk}} = h\nu_{\text{pk}}/(m_e c^2) = 10^{-6} \epsilon_{-6}$ requires a magnetic field of

$$B = 9 \left(\frac{D}{10} \right)^{-1} \frac{d_{27}^{4/7} f_{-10}^{2/7} \epsilon_B^{2/7}}{(1+z)^{4/7} \epsilon_{-6}^{1/7} R_{15}^{6/7} (p-2)^{2/7}} \text{ G}, \quad (1)$$

where d_{27} is the luminosity distance in units of 10^{27} cm, ϵ_B is the magnetic-field equipartition factor, and R_{15} is R_B in units of 10^{15} cm. For $d_{27} = 1.45$, $f_{-10} \sim 1$, $\epsilon_B \sim 1$ (corresponding to equipartition), $\epsilon_{-6} \sim 1$ (corresponding to a peak frequency in the near infrared), $R_{15} = 10$, and $p \sim 2.5$, we find $B_{\text{ep}} \sim 1.8$ G, which is within a factor of ~ 2 of the values quoted in Tab. 2. The above value of B_{ep} implies a synchrotron cooling time scale (in the observer's frame) of electrons emitting synchrotron radiation at an observed energy $E_{\text{sy}} = 1 E_{\text{keV}}$ keV of

$$\tau_{\text{sy}} \approx 0.12 \left(\frac{B}{1.8 \text{ G}} \right)^{-3/2} \left(\frac{D}{10} \right)^{-1/2} E_{\text{keV}}^{-1/2} \text{ hr}. \quad (2)$$

which, for X-ray photon energies, is shorter than the dynamical time scale $R_B/(Dc)$, in agreement with the approximately symmetric shape of the X-ray light curves. Since the

optical – γ -ray spectrum constitutes a time-average over a time scale of $\tau \gtrsim 20$ hr, we expect to observe the time-averaged emission from a strongly cooled electron population down to synchrotron energies of

$$E_c = 3.5 \times 10^{-2} \tau_{20}^{-2} \left(\frac{B}{1.8 \text{ G}} \right)^{-3} \left(\frac{D}{10} \right)^{-1} \text{ eV}, \quad (3)$$

which is in the infrared range. In Eq. (3), $\tau_{20} = \tau/(20 \text{ hr})$. If additional electron cooling mechanisms play a significant role (see §5), the cooling time scale τ_c will obviously be shorter than τ_{sy} , further strengthening the argument for time-averaged emission observed beyond infrared frequencies.

4. Spectral Modeling Results and Predictions for VHE emission

Since the EGRET detection of W Comae during May 1998 was of rather low significance (see §2) and not quite simultaneous to the *BeppoSAX* observation, and in view of the uncertainty of the source identification, we first focus on the simultaneous optical – X-ray spectrum. As the simplest possible variation of the leptonic jet model, we attempt to model this spectrum using a strongly SSC-dominated model in which we neglect any soft-photon input from the broad line region (i.e., we set $\tau_{\text{T,BLR}} = 0$). As a first guess, we fix a bulk Lorentz factor of $\Gamma = 10$, yielding $D = 19.41$. We then start out by choosing an arbitrary value of γ_1 , and try to adjust the model parameters γ_2 , p , and n_e so that a good fit to the optical – X-ray spectrum of W Comae is achieved. We find that this is possible for values of $500 \lesssim \gamma_1 \lesssim 2000$. The curves no. 1 – 5 in Fig. 3 illustrate the resulting model fits for a sequence of models with γ_1 in the above range. For substantially lower values of γ_1 , our model spectra become too flat to join the optical and X-ray spectra. The model parameters for each simulation are listed in Table 2. The last column in Table 2 lists the integrated photon fluxes from those models at energies $E > 40$ GeV. The table indicates that different SSC model fits to the optical – X-ray spectrum of W Comae predict levels of VHE emission which differ by a factor of more than 10.

In a second step, we investigate how much our results depend on the (rather arbitrary) choice of $\Gamma = 10$ adopted above. To this aim, we now fix an intermediate value of $\gamma_1 = 1000$ from the previous models, and attempt to find model fits for different values of Γ . Specifically, we repeat the fitting procedure for $\Gamma = 4$ and $\Gamma = 15$, corresponding to $D = 7.78$, and $D = 28.05$, respectively. Again, we do not encounter any fundamental problem in finding appropriate model parameters to provide a good fit to the optical – X-ray spectrum of W Comae. Similar to the previous series of fits, the two new model fits predict levels of

VHE emission differing by about an order of magnitude. The fit results are shown as curves no. 6 and 7 in Fig. 3

Fig. 3 illustrates another very interesting result: Although the different SSC model fits predict very different levels of > 40 GeV emission, they all cut off around 100 GeV. Thus, no > 100 GeV emission is predicted by any of our model fits. This is related to the high-energy cut-off of the synchrotron component, which is very well constrained by the high-quality X-ray spectrum observed by *BeppoSAX*. Table 2 indicates that there is a certain degree of anti-correlation between γ_1 and γ_2 . As mentioned above, the minimum allowed value for γ_1 is rather well defined so that we do not have the freedom to choose very low values of γ_1 in order to attempt to find acceptable fits with very large values of γ_2 which would be able to produce substantially higher VHE cutoffs.

As pointed out by Tagliaferri et al. (2000), a pure SSC model fit to the 1998 SED of W Comae produces a γ -ray spectrum which is incompatible with the EGRET spectrum if the spectral index resulting from this low-significance detection is to be trusted. The fact that EGRET detections of the source during other viewing periods yielded similar spectral shapes in the 0.1 – 10 GeV regime (§2) provides some circumstantial evidence that there might indeed be a separate high-energy emission component producing a spectral bump centered at a peak energy of $E_{\text{pk,HE}} \gtrsim 10$ GeV. In the framework of our generic leptonic jet model, this can be plausibly related to an external Compton component. In Fig. 4, we illustrate, how the overall spectral shape of our model fit no. 1 (see Fig. 3 and Tab. 2) changes if an external Compton component due to soft photons reprocessed in the broad line region is included in the model. The radio – hard X-ray emission from the different models remains virtually invariant under the inclusion of the EC component. The EGRET spectrum can be very well accommodated assuming a radial Thomson depth of our model BLR of $\tau_{\text{T,BLR}} \sim 3 \times 10^{-3}$. This would raise the predicted > 40 GeV flux from the model by a factor of ~ 3 compared to the pure SSC model with otherwise identical parameters. The sharp cut-off of the VHE emission around ~ 100 GeV remains unchanged even with the inclusion of the EC component. The low-energy cut-off of the external-Compton component is caused by the sharp cut-off in the electron injection function at γ_1 . This cut-off is maintained in the evolving electron distribution throughout the simulation because the radiative cooling time scale for electrons of energy $\gamma \lesssim \gamma_1$ is much longer than the dynamical time scale for the parameters used here.

From this analysis, we can conclude that pure spectral modeling of the optical – X-ray emission of W Comae is insufficient to make reliable predictions about the expected level of VHE emission at > 40 GeV from this object. In the next section, we illustrate, how the combination of spectral and X-ray variability information can be used to put significantly

tighter constraints on the expected level of VHE emission — even without independent information about the γ -ray emission.

5. X-ray variability

Apart from the spectral information, the *BeppoSAX* X-ray observations of May 1998 revealed variability in the soft band (0.1 – 4 keV), dominated by a broad flare with a rise time of ~ 7 hr and a decay time of ~ 10 hr (see Fig. 2 of Tagliaferri et al. (2000)), corresponding to ~ 6 hr and ~ 9 hr in the cosmological rest-frame of the source. In the hard band (4 – 10 keV), no significant variability was detected. Because of the limited photon statistics, local spectral indices or hardness ratios within the soft and hard bands could not be extracted with useful temporal resolution. However, such information might become available through observations with the new generation of X-ray telescopes, in particular *XMM-Newton* and *Chandra*. For this reason, we are now investigating generic light curves and spectral variability signatures at X-rays resulting from the different model fits to W Comae presented in the previous section.

To do so, we use a code which is based on the jet radiation transfer code of Böttcher et al. (1997) and Böttcher & Bloom (2000), but accounts for time-dependent electron acceleration and/or injection throughout the evolution of the emitting region as it moves outward along the jet. A detailed code description as well as a parameter study for various generic model situations will be presented in Böttcher & Chiang (2002). The numerical approach is very similar to the one used by Li & Kusunose (2000) who had investigated the broadband spectral variability features in a pure SSC model for flaring blazars, but our code allows for the additional electron cooling and photon emission from external Compton scattering (both direct accretion-disk photons and accretion-disk emission reprocessed in the broad-line region) and takes into account $\gamma\gamma$ absorption intrinsic to the source, including the corresponding pair production.

In order to investigate a generic spectral-variability model for W Comae, we assume that the electron injection during a flare occurs at a constant rate over one dynamical time scale $t_{\text{dyn}} = R_B/c$ in the co-moving frame, and then proceeds at a lower rate, corresponding to the quiescent emission outside the flaring episode. Consequently, the parameters pertaining to the relativistic electron distributions quoted in Table 2 correspond to flaring injection luminosities of $L_{\text{inj}}^{\text{fl}} = 3 \times 10^{41}$ ergs s^{-1} (fit no. 1) to $L_{\text{inj}}^{\text{fl}} = 2.6 \times 10^{42}$ ergs s^{-1} (fit no. 5). We choose a quiescent injection luminosity of $L_{\text{inj}}^{\text{qu}} = 10^{40}$ ergs s^{-1} .

Fig. 5 illustrates the time-dependent photon spectra resulting from these simulations

corresponding to the spectral fits no. 1 (SSC model with the lowest SSC flux of the fits shown in Fig. 3), 5 (SSC model with the highest SSC flux of the fits shown in Fig. 3), and 10 (complete SSC + EC model with the largest EC contribution of the fits shown in Fig. 4). Fig. 6 shows the light curves in the R-band and at 4 different X-ray energies resulting from the same time-dependent simulations. The figure illustrates that the light curves corresponding to the fits no. 1 and 5 are qualitatively very different. The almost symmetric shape of the observed light curve is clearly not reproduced by the SSC dominated case no. 5. However, no significant difference in the optical and X-ray light curves results from the inclusion of an EC component, even in the most extreme case of spectral fit no. 10 (with $\tau_{\text{T,BLR}} = 10^{-2}$). Note, however, that even in this case the bolometric luminosity (and, consequently, the electron cooling) is still dominated by the synchrotron component, which may explain the fact that it has only a negligible impact on the low-frequency light curves.

In Fig. 7, we show tracks in the hardness-intensity diagrams (monoenergetic flux, normalized to the peak flux, vs. energy spectral index α), produced in the different model situations. As with the light curves shown in Fig. 6, the synchrotron dominated case no. 1 should be clearly distinguishable from the SSC dominated case no. 5, while the inclusion of an EC component leaves the hardness-intensity tracks virtually unchanged.

In the simulations above, we have assumed the simplest possible time-dependence of the electron acceleration, namely a step function. Li & Kusunose (2000) have also touched on the issue of different intrinsic injection functions, and found the effect on the light curves is only of minor importance, if the total duration of the flare injection event is of the same order of magnitude as the dynamic time scale, and the total injected energy remains unchanged. From this, we may conclude that our results do not strongly depend on the detailed shape of the injection profile, at least to the degree of accuracy with which the soft X-ray variability could be measured by *BeppoSAX*.

In summary, our modeling results indicate that cooling of the ultrarelativistic electron and/or pair plasma in the jet is synchrotron and/or EC dominated. The most realistic model parameters therefore seem to be close to the simulations no. 1 or 2, with a possible moderate contribution due to external Compton scattering, depending on whether the observed EGRET flux from 3EG J1222+2841 is indeed related to W Comae. Consequently, we predict a > 40 GeV flux from W Comae of $\sim (0.4 - 1) \times 10^{-10}$ photons $\text{cm}^{-2} \text{s}^{-1}$ with no significant emission at $E \gtrsim 100$ GeV. Note, however, that our conclusions about the X-ray variability have so far only been based on the soft X-ray light curve measured by *BeppoSAX*. We strongly suggest that our predictions about the energy-dependent hardness-intensity variability illustrated in Fig. 7 should be tested with future observations by *XMM-Newton* or *Chandra*.

6. Comparison to hadronic models

An alternative to leptonic models are the so-called "hadronic models" proposed to explain γ -ray emission from blazars. While leptonic models deal with a relativistic e^\pm plasma in the jet, in hadronic models the relativistic jet consists of a relativistic proton (p) and electron (e^-) component. Here we use the hadronic Synchrotron-Proton Blazar (SPB-) model of Mücke et al. (2002) to model the spectral energy distribution (SED) of W Comae in May 1998.

Like in the leptonic model the emission region, or "blob", in an AGN jet moves relativistically along the jet axis which is closely aligned with our line-of-sight. Relativistic (accelerated) protons, whose particle density n_p follows a power law spectrum $\propto \gamma_p^{-\alpha_p}$ in the range $2 \leq \gamma_p \leq \gamma_{p,\max}$, are injected instantaneously into a highly magnetized environment ($B = \text{const}$ within the emission region), and suffer energy losses due to proton-photon interactions (meson production and Bethe-Heitler pair production), synchrotron radiation and adiabatic expansion. The mesons produced in photon-meson interactions always decay in astrophysical environments, however, they may suffer synchrotron losses before the decay, which is taken into account in this model.

The relativistic primary e^- radiate synchrotron photons that manifest themselves in the blazar SED as the synchrotron hump, and serve as the target radiation field for proton-photon interactions and the pair-synchrotron cascade which subsequently develops. The SPB-model is designed for objects with a negligible external target photon component, and hence suitable for BL Lac Objects. The cascade redistributes the photon power to lower energies where the photons eventually escape from the emission region. The cascades can be initiated by photons from π^0 -decay (" π^0 cascade"), electrons from the $\pi^\pm \rightarrow \mu^\pm \rightarrow e^\pm$ decay (" π^\pm cascade"), p -synchrotron photons (" p -synchrotron cascade"), charged μ^- , π^- and K -synchrotron photons (" μ^\pm -synchrotron cascade") and e^\pm from the proton-photon Bethe-Heitler pair production (" $\text{Bethe-Heitler cascade}$ ").

Mücke & Protheroe (2001) and Mücke et al. (2002) have shown that the " π^0 cascades" and " π^\pm cascades" generate rather featureless photon spectra, in contrast to " p -synchrotron cascades" and " μ^\pm -synchrotron cascades" that produce a double-humped SED as typically observed for γ -ray blazars. The contribution from the Bethe-Heitler cascades is mostly negligible. In general direct proton and muon synchrotron radiation is mainly responsible for the high energy hump in blazars whereas the low energy hump is dominated by synchrotron radiation from the primary e^- , with a contribution of synchrotron radiation from secondary electrons (produced by the p - and μ^\pm -synchrotron cascade). A detailed description of the model itself, and its implementation as a (time-independent) Monte-Carlo/numerical code, has been given in Mücke & Protheroe (2001).

For the modeling of the 1998 SED of W Comae we have fixed the effective size scale of the emission region to $R_b = \frac{1}{2}ct_{\text{var}}D$ where $t_{\text{var}} \approx 10\text{h}$ is the measured soft X-ray variability time scale. We consider bulk Doppler factors in the range $D = 5 - 20$ for the fitting procedure, which is consistent with the moderate superluminal motion detected by Massaro et al. (2001). The primary relativistic electrons emit synchrotron photons, which serve as the target photon field for photon-proton interactions and cascading. The synchrotron spectrum from these electrons shows a break at around 10^{13} Hz where the synchrotron cooling time scale $t_{e,\text{syn}} \approx 8 \times 10^8 (B/1\text{G})^{-2} \gamma^{-1}$ sec equals the adiabatic loss time scale $t_{\text{ad}} \approx \xi R_b/c$ for a relativistic jet with $\xi \leq 1$, taking into account a possible non-spherical geometry, effects of a possible accelerating (i.e. non-constant speed) jet, etc. In the soft X-ray regime, the spectrum turns over steeply when the cooling time scale becomes shorter than the acceleration time scale $t_{\text{acc}} = r_L/(\eta c)$ ($r_L =$ Larmor radius, $\eta \leq 1 =$ acceleration efficiency). Note that the theory of plasma turbulence predicts significantly lower η values for electrons than for protons.

Fig. 8 shows a summary of SPB-models best representing the March/May 1998 data. Similar to the leptonic SSC model, the SPB-model seems to be not compatible with the March 1998 EGRET data if the May 1998 LECS + MECS + PDS data from BeppoSAX are modeled (see models 3 – 5). On the other hand, the BeppoSAX LECS + MECS data together with the EGRET spectrum can be explained by hadronic models (see models 1 + 2), which however underestimate the flux in the PDS energy band by about a factor of 3. The non-compatibility of the EGRET- with the BeppoSAX-data in the modeling procedure might be caused by their non-simultaneity and the poor significance of the EGRET-detection. Note also that during the May 1998 BeppoSAX observing run some technical problems occurred which might have affected the PDS data (Tagliaferri et al. 2000).

In the framework of the hadronic SPB-model the hard X-ray spectrum can naturally be explained by strong synchrotron emission from the relativistic protons provided strong magnetic fields B of several tens of Gauss exist in the emission region. For the modeling (models 3 – 5) we use $B = 30 - 40$ G, $\alpha_p = 1.5$, $\gamma_{p,\text{max}} = 5 - 10 \times 10^8$, a number density ratio of primary, relativistic electrons to protons, $e/p \approx 0.1$, and a proton energy density $u_p \approx 60 - 150$ ergs cm^{-3} , somewhat above the equipartition value, which is not surprising during activity in the source. With Doppler factors $D = 12 - 15$ the target photon energy density in the jet frame is $\sim 10^{10} - 10^{11}$ eV cm^{-3} . Because proton synchrotron losses dominate in the high energy region over pion production losses (see Fig. 11), the model predicts the main power output at several 100 MeV due to proton synchrotron radiation, with a strong steepening by about 2 orders of magnitude in the GeV range, and γ -ray emission from the π -cascades extending up to about 100 TeV with a break at about 10 TeV at the source. Photons above ~ 100 GeV (in the co-moving frame) will be subject to $\gamma\gamma$ absorption within

the emission region, and initiate electromagnetic cascades in the jet (see Fig. 12). Absorption of multi-GeV/TeV-photons in the cosmic background radiation field will further alter the observed spectrum: the optical depth exceeds unity above 300 – 700 GeV for W Comae. The predicted photon flux above 40 GeV (see Tab. 3) is therefore similar to the corresponding predictions from the leptonic models (see Tab. 2).

If the intrinsic target photon density increases to $\sim 10^{11} - 10^{12} \text{ eV cm}^{-3}$, muon and pion production, and therefore also muon and pion synchrotron radiation, dominates over proton synchrotron radiation (see Fig. 11). This might have been the case during the EGRET-observations (see Fig. 8: model 1 + 2, and Fig. 10). Because pions and muons possess a lower rest mass with respect to protons, their synchrotron emission peaks at higher photon energies than the protons' synchrotron radiation for the same particle Lorentz factors and magnetic fields. The parameters used for the models representing the EGRET data (models 1 + 2) are: $D = 8 - 10$, $B = 40 \text{ G}$, $\alpha_p = 1.5 - 2$, $\gamma_{p,\text{max}} = (1 - 3) \times 10^9$, $e/p \approx 0.2 - 1.6$ and a proton energy density $u_p \approx 250 - 300 \text{ ergs cm}^{-3}$. The main power output in the high-energy regime for models 1 + 2 lies therefore at $\sim 10 \text{ GeV}$, and is somewhat higher at IR-energies. For these parameters, photons beyond a few tens of GeV (in the co-moving frame) will be subject to $\gamma\gamma$ absorption, and initiate electromagnetic cascades (see Fig. 12). Also here, the model predicts TeV-emission from the π -cascades (however not extending above 1 TeV), which however will partly be absorbed in the cosmic photon background.

Models involving meson production inevitably predict neutrino emission due to the decay of charged mesons. The SPB-model for W Comae in 1998 predict a $\nu_\mu + \bar{\nu}_\mu$ output of about $10^{-7} \text{ GeV s}^{-1} \text{ cm}^{-2}$ peaking at around $10^{8.5-9} \text{ GeV}$. The neutrino power at 10^6 GeV is about $10^{-11 \dots -10} \text{ GeV cm}^{-2} \text{ s}^{-1}$. No neutrino flavor oscillations are assumed here.

In summary, the hadronic SPB-model predicts TeV-emission on a flux level near the detectability capabilities of CELESTE and STACEE for W Comae, but clearly above the sensitivity limit of future instruments like VERITAS. While leptonic models predict integral fluxes at $> 40 \text{ GeV}$ for W Comae on a similar level than hadronic models do, TeV-emission detectable with very high-sensitivity instruments is only predicted for the hadronic emission processes. This is in contrast to leptonic models, and may therefore be useful as a diagnostic to distinguish between the hadronic and leptonic nature of the high-energy emission from W Comae, in addition to its possible neutrino emission.

7. Summary

We have presented detailed modeling of the best currently available simultaneous broadband SED of the radio-selected BL Lac object W Comae, comparing state-of-the-art leptonic and hadronic jet models. The richest and most detailed portion of the SED consists of the BeppoSAX LECS + MECS + PDS spectrum from $\sim 0.1 - 100$ keV, measured in May 1998 (Tagliaferri et al. 2000). It showed the low-energy (synchrotron) component extending out to ~ 4 keV, exhibiting significant variability on time scales of $\lesssim 10$ hr, and the onset of the high-energy component beyond ~ 4 keV, with no evidence for short-term variability. The SED was supplemented by simultaneous radio and optical flux measurements as well as a weak EGRET detection in March 1998, i. e. about 2 months before the BeppoSAX spectrum was taken. We have done a careful re-analysis of all available EGRET pointings on W Comae, and confirmed that the source exhibited an unusually hard GeV spectrum during the March 1998 observation, with a photon spectral index of $\alpha = 1.27 \pm 0.58$.

Our fits using leptonic jet models yielded the following main results:

(1) Acceptable fits to the optical to hard X-ray spectrum of W Comae are possible with a rather wide range of parameters in a synchrotron-self-Compton (SSC) dominated model. In agreement with earlier results of Tagliaferri et al. (2000), we find that such fits are generally inconsistent with the (not quite simultaneous) EGRET spectrum of March 1998 as well as the average spectrum over the entire lifetime of EGRET.

(2) The different SSC fits to the optical – hard X-ray spectrum of W Comae in May 1998 result in > 40 GeV fluxes of $\sim (0.4 - 4) \times 10^{-10}$ photons $\text{cm}^{-2} \text{s}^{-1}$, but virtually no emission beyond ~ 100 GeV.

(3) Including the information contained in the X-ray variability measured by BeppoSAX, we can narrow down the range of possible leptonic model parameters to predict > 40 GeV fluxes of $\sim (0.4 - 1) \times 10^{-10}$ photons $\text{cm}^{-2} \text{s}^{-1}$.

(4) In order to reproduce the March 1998 EGRET spectrum together with the May 1998 BeppoSAX spectrum, an external Compton component is required. Such fits result in > 40 GeV fluxes of $\sim (0.5 - 1) \times 10^{-10}$ photons $\text{cm}^{-2} \text{s}^{-1}$, and a strong cutoff at $\lesssim 100$ GeV, as in the case of SSC dominated models.

Successful fits to the SED of W Comae were also possible using the hadronic Synchrotron-Proton Blazar model, yielding the following main results:

(5) A model with proton-synchrotron dominated hard X-ray to GeV γ -ray emission is well suited to reproduce the entire radio – hard X-ray spectrum of W Comae in May 1998. Just as the SSC-dominated leptonic models, it is inconsistent with both the March 1998 and

the average EGRET spectrum from the source.

(6) The hadronic fit to the radio – hard X-ray spectrum of W Comae predicts a > 40 GeV flux of $\sim (0.7 - 1.4) \times 10^{-10}$ photons $\text{cm}^{-2} \text{s}^{-1}$, i.e. of the same order as the predictions of the leptonic jet models. However, in contrast to the leptonic models, the high-energy emission is expected to extend beyond 1 TeV at a flux level of $\Phi_{>1 \text{ TeV}} \sim (3 - 18) \times 10^{-14}$ photons $\text{cm}^{-2} \text{s}^{-1}$. Such a flux level is well within the reach of future high-sensitivity instruments like VERITAS.

(7) SPB models consistent with the March 1998 EGRET spectrum under-predict the May 1998 BeppoSAX PDS hard X-ray spectrum. They result in higher > 40 GeV fluxes of $\sim (5 - 13) \times 10^{-10}$ photons $\text{cm}^{-2} \text{s}^{-1}$, but weaker TeV fluxes of $\Phi_{>1 \text{ TeV}} \sim (0.7 - 9) \times 10^{-14}$ photons $\text{cm}^{-2} \text{s}^{-1}$. In this case, STACEE and CELESTE may be able to get a weak detection of the source, and it would still be a promising candidate for detection by the future VERITAS array.

In conclusion, leptonic and hadronic jet model fits to W Comae make drastically different predictions with respect to the expected very-high energy emission beyond ~ 100 GeV. A detection of W Comae at those photon energies with future, high-sensitivity air Čerenkov detector arrays would pose a serious challenge to leptonic jet models, and might favor hadronic models instead.

We thank D. Smith for inspiring discussions, and G. Ghisellini for making the data on the May 1998 SED of W Comae available to us. We are also grateful to J. Chiang for careful reading of the manuscript and helpful comments. The work of MB was supported by NASA through Chandra Postdoctoral Fellowship grant PF 9-10007 awarded by the Chandra X-ray Center, which is operated by the Smithsonian Astrophysical Observatory for NASA under contract NAS 8-39073. RM acknowledges support from NSF grant PHY-9983836. AR thanks the Bundesministerium für Bildung und Forschung for financial support through DESY grant Verbundforschung 05CH1PCA6.

REFERENCES

- Aharonian, F. A., 2001, in: Proc. 27th Int. Cosmic Ray Conf., Hamburg/Germany
- Aharonian, F. A., & Akerlof, C. W., 1997, *Ann. Rev. Nucl. Part. Sci.* 47, 273
- Blandford, R. D., & Levinson, A., 1995, *ApJ*, 441, 79
- Bloom, S. D., & Marscher, A. P., 1996, *ApJ*, 461, 657

- Böttcher, M., Mause, H., & Schlickeiser, R., 1997, *A&A*, 324, 395
- Böttcher, M., Aller, H. D., Aller, M. F., Mang, O., Raiteri, C. M., Ravasio, M., Tagliaferri, G., Teräsanta, H., & Villata, M., 2002, in proc. “Blazar Astrophysics with BeppoSAX and other Observatories”, special ASI public., Eds. P. Giommi, E. Massaro, & G. Palumbo, in press
- Böttcher, M., & Bloom, S. D., 2000, *AJ*, 119, 469
- Böttcher, M., & Chiang, J., 2002, *ApJ*, submitted
- Chiang, J., & Böttcher, M., 2002, *ApJ*, 564, 92
- Coppi, P. S., & Aharonian, F. A., 1999, *ApJ*, 521, L33
- Costamante, L., & Ghisellini, G., 2002, *A&A*, 384, 56
- de Jager, O., & Stecker, F. W., 2002, *ApJ*, 566, 738
- Dermer, C. D., Schlickeiser, R., & Mastichiadis, A., 1992, *A&A*, 256, L27
- Dermer, C. D., & Schlickeiser, R., 1993, *ApJ*, 416, 458
- Dermer, C. D., Sturmer, J. J., & Schlickeiser, R., 1997, *ApJS*, 109, 103
- Dingus, B. L., & Bertsch, D. L., 2001, *AIP conf. proc.* 587, 251 Eds.: S. Ritz, N. Gehrels, & C. R. Shrader
- Hartman, R. C., et al., 1999, *ApJS*, 123, 79
- Kerrick, A. D., et al., 1995, *ApJ*, 452, 588
- Konopelko, A., 1999, *Astropart. Phys.*, 11, 263
- Lamb, R. C., & Macomb, D. J., 1997, *ApJ*, 488, 872
- Li, H., & Kusunose, M., 2000, *ApJ*, 536, 729
- Maisack, M., et al., 1997, in Proc. of “Conf. on Blazars, Black Holes, and Jets”, Girona, Spain, 9 - 12 Sept. 1996, Eds. M. Kidger, & J. A. de Diego, *Astrophysics and Space Science*
- Mannheim, K., 1996, *Space Sci. Rev.*, 75, 331
- Maraschi, L., Celotti, A., & Ghisellini, G., 1992, *ApJ*, 397, L5

- Marscher, A. P., & Gear, W. K., 1985, *ApJ*, 298, 114
- Massaro, E., Mantovani, F., Fanti, R., Nesci, R., Tosti, G., & Venturi, T., 2001, *A&A*, 374, 435
- Mattox, J. R., et al., 1996, *ApJ*, 461, 396
- Mattox, J. R., Hartman, R. C., & Reimer, O., 2001, *ApJS*, 135, 155
- Melia, F. & Königl, A., 1989, *ApJ*, 340, 162
- Mücke, A. & Protheroe, R.J., 2001, *Astropart. Phys*, 15, 121
- Mücke, A., Protheroe, R.J., Engel, R., Rachen, J.P. & Stanev, T. 2002, *Astropart. Phys*, in press (astro-ph/0206164)
- Nolan, P. L., et al., 1993, *ApJ*, 409, 697
- Ong, R., et al., 2001, in *Proc. of the XXVII ICRC*
- Sikora, M., Begelman, M., & Rees, M. J., 1994, *ApJ*, 421, 153
- Smith, D., A., 2002, *Proc. of “Blazar Astrophysics with BeppoSAX and other Observatories”*, Special ASI Publication, Eds. P. Giommi, E. Massaro, & G. Palumbo, in press
- Sreekumar, P., et al., 1996, *ApJ*, 464, 628
- Stecker, F. W., de Jager, O. C., & Salamon, M. H., 1996, *ApJ*, 473, L75
- Tagliaferri, G., et al., 2000, *A&A*, 354, 431
- Theoret, C., 2000, Ph.D. Thesis, McGill University
- Thompson, D. J., et al., 1993, *ApJ*, 415, L13
- von Montigny, C., et al., 1995, *ApJ*, 440, 525
- Weekes, T. C., et al., *Astropart. phys.*, 17, 221
- Wolter, A., Tavecchio, F., Caccianiga, A., Ghisellini, G., & Tagliaferri, G., 2000, *A&A*, 357, 429

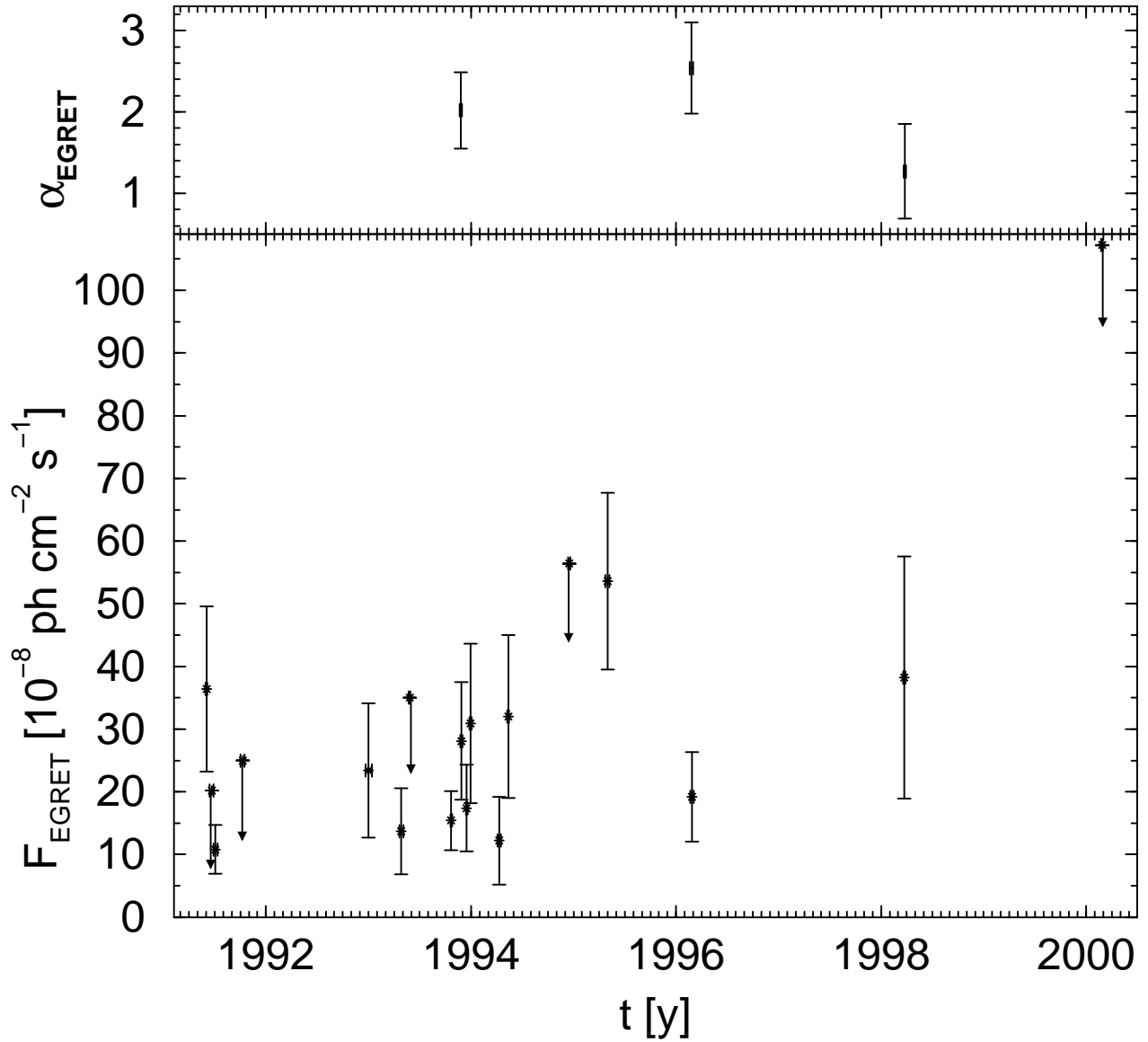


Fig. 1.— Lower panel: EGRET light curve of W Comae over the entire lifetime of the *Compton Gamma-Ray Observatory*. Upper panel: Best-fit spectral indices (photon indices) of some of the most significant EGRET detections.

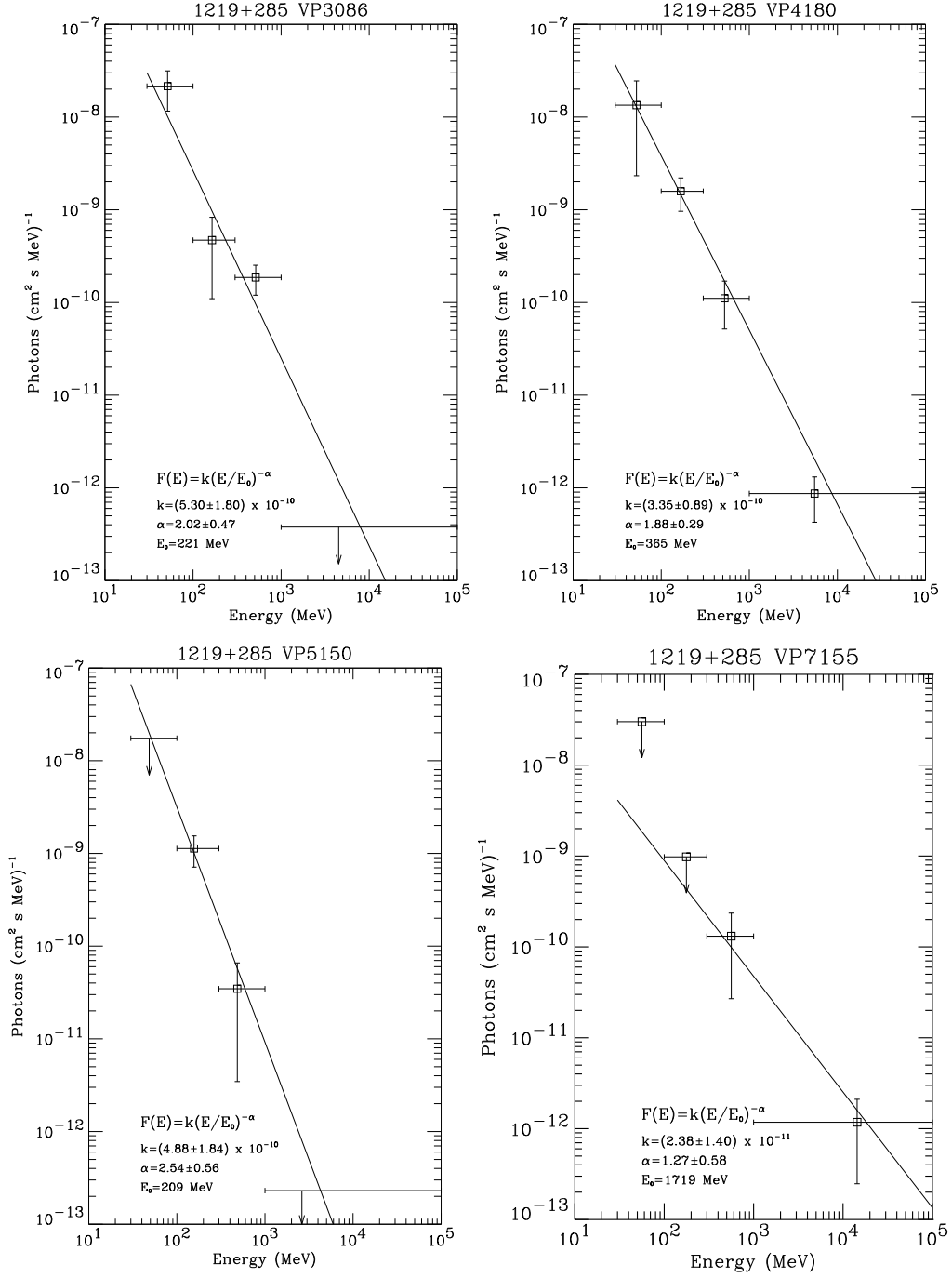


Fig. 2.— 4-point EGRET spectra during the most significant EGRET detections of W Co-mae. The lines show the power-law fits to those spectra.

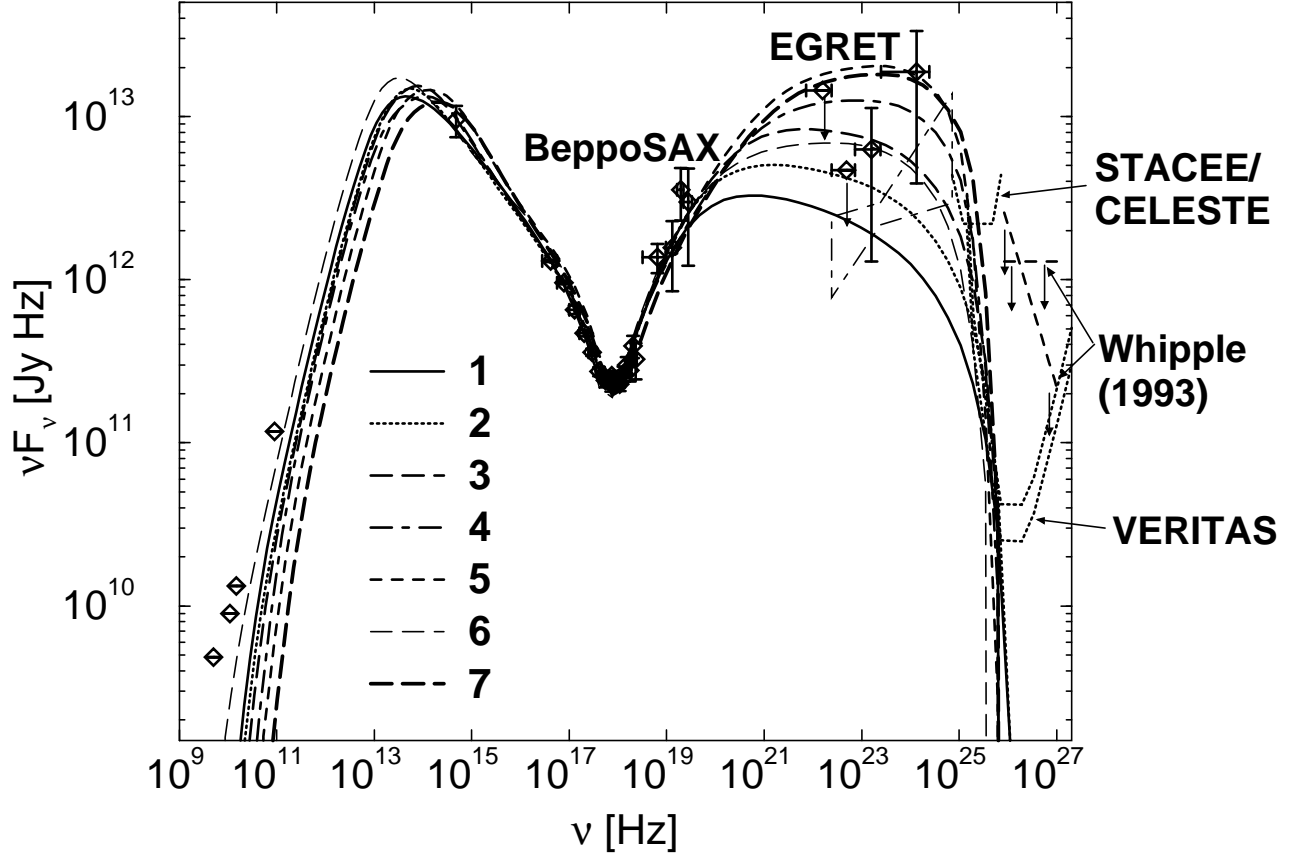


Fig. 3.— Various model fits to the optical – X-ray spectrum of W Comae in May 1998, using a pure SSC model. The radio – X-ray spectral data points from Tagliaferri et al. (2000); the EGRET data points are the result of our re-analysis of the March 1998 observation. The dot-dashed bow-tie outline shows the average EGRET spectrum from the 3rd EGRET catalogue (Hartman et al. 1999). Also shown are the sensitivities of current and future ACTs as well as the upper limit from the Whipple observation in 1993. The two different sensitivity curves for VERITAS result from assuming an underlying power-law photon spectrum of index $\alpha = 2.5$ and $\alpha = 3.5$, respectively. For fits no. 1 - 5, we have fixed the Doppler boosting factor $D = 19.41$, changed the low-energy cutoff of the electron distribution from $\gamma_1 = 500$ to 1600, and adjusted the remaining parameters to achieve an acceptable fit to the optical – X-ray spectrum. For fits 6, 3, and 7, we fixed $\gamma_1 = 1000$, changed the Doppler boosting factor from $D = 7.78$ to 28.05, and adjusted the remaining parameters to achieve a good fit. For the complete list of parameters, see Table 2.

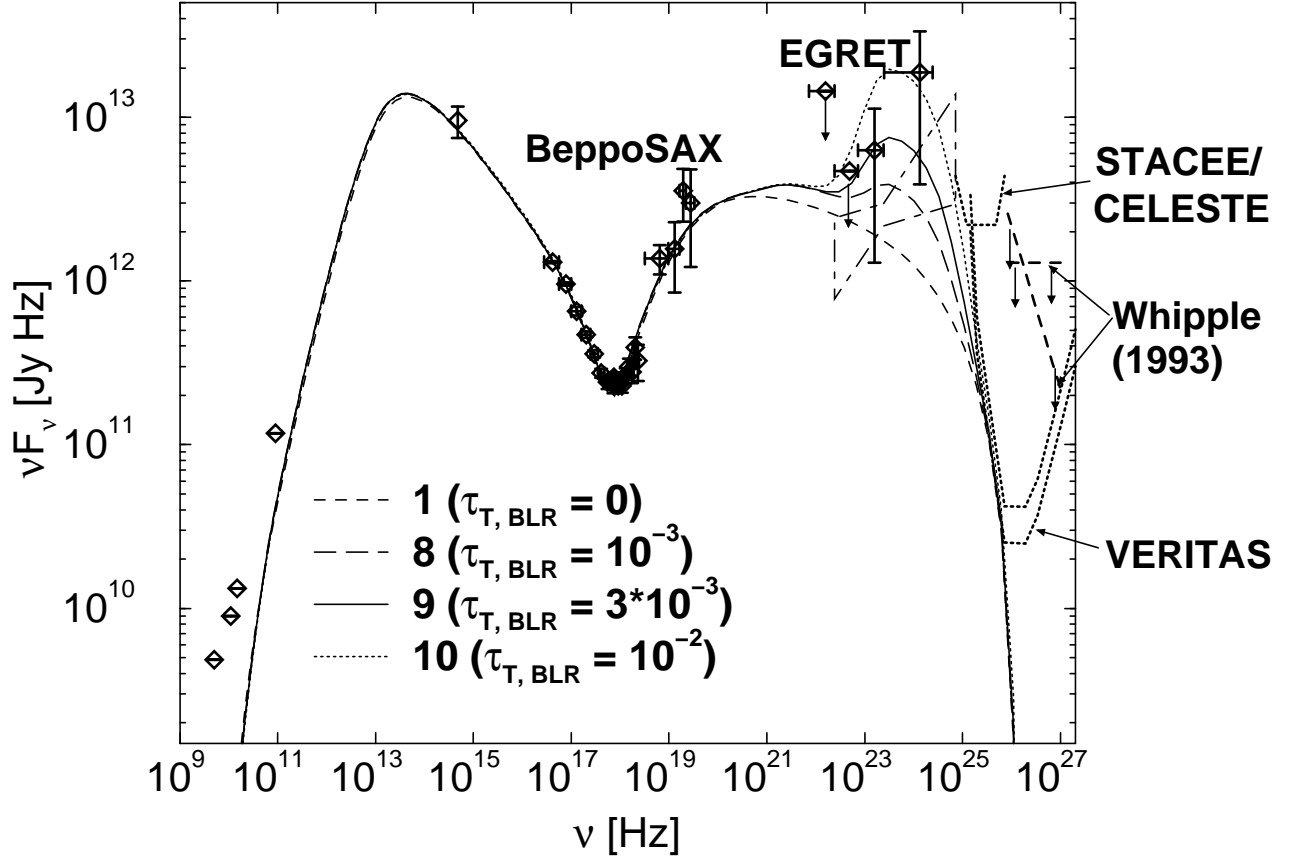


Fig. 4.— Various model fits to the optical – X-ray spectrum of W Comae in 1998, using an SSC + ERC model. The choice of parameters is based on fit no. 1 in Fig. 3, but additionally accounting for an increasing amount of reprocessed accretion disk radiation in a broad line region of radial Thomson depth $\tau_{\text{BLR}} = 0$ to 10^{-2} . For the complete list of parameters, see Table 2.

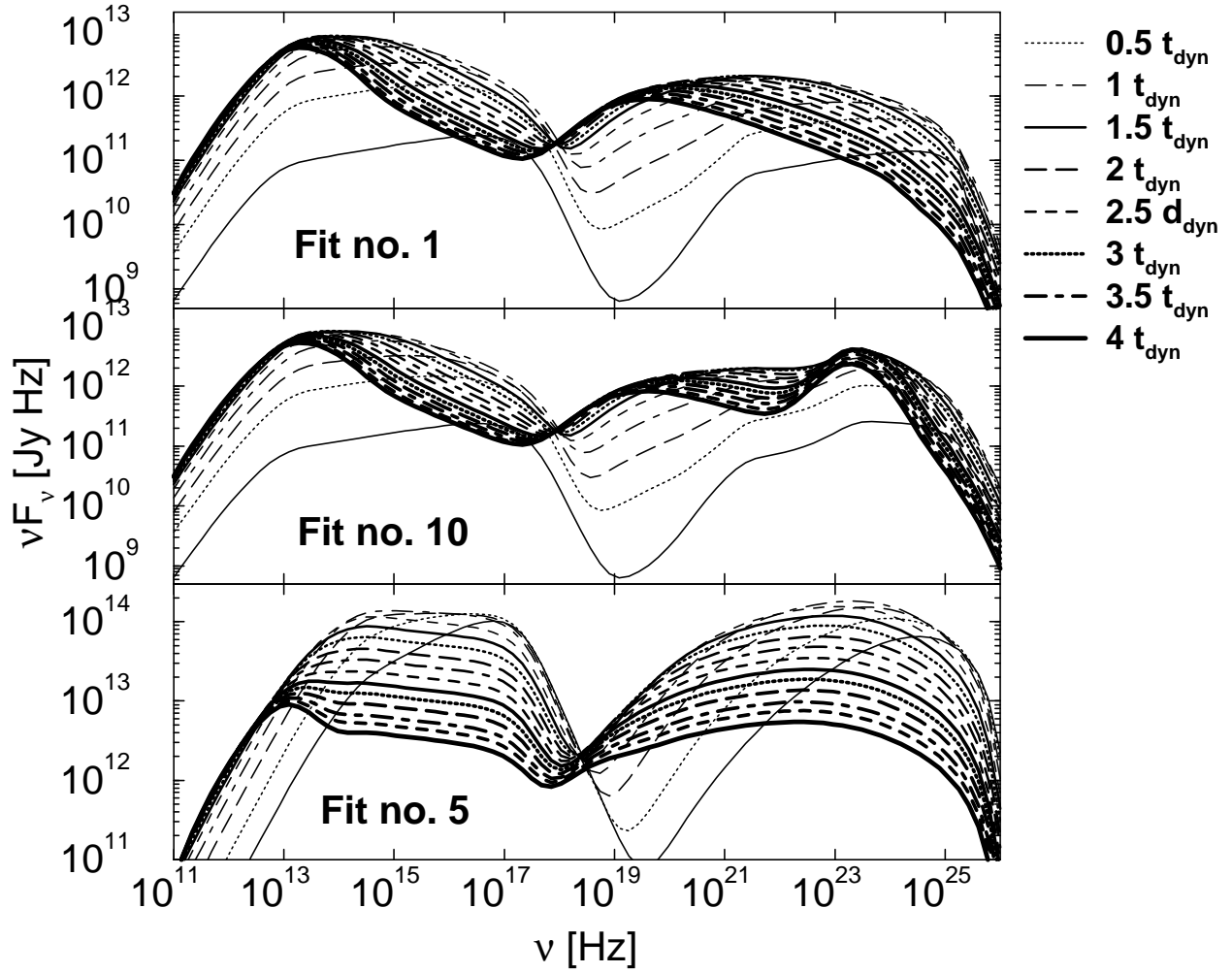


Fig. 5.— Simulated, time-dependent broad-band spectra corresponding to the spectral fits no. 1, 5, and 10 (see Figs. 3 and 4 and Tab. 2). The curves are labeled by time in units of the dynamical time scale, $R_b/(Dc)$, which is $t_{dyn}^{obs} = 1.8 \times 10^4$ s in the observer’s frame.

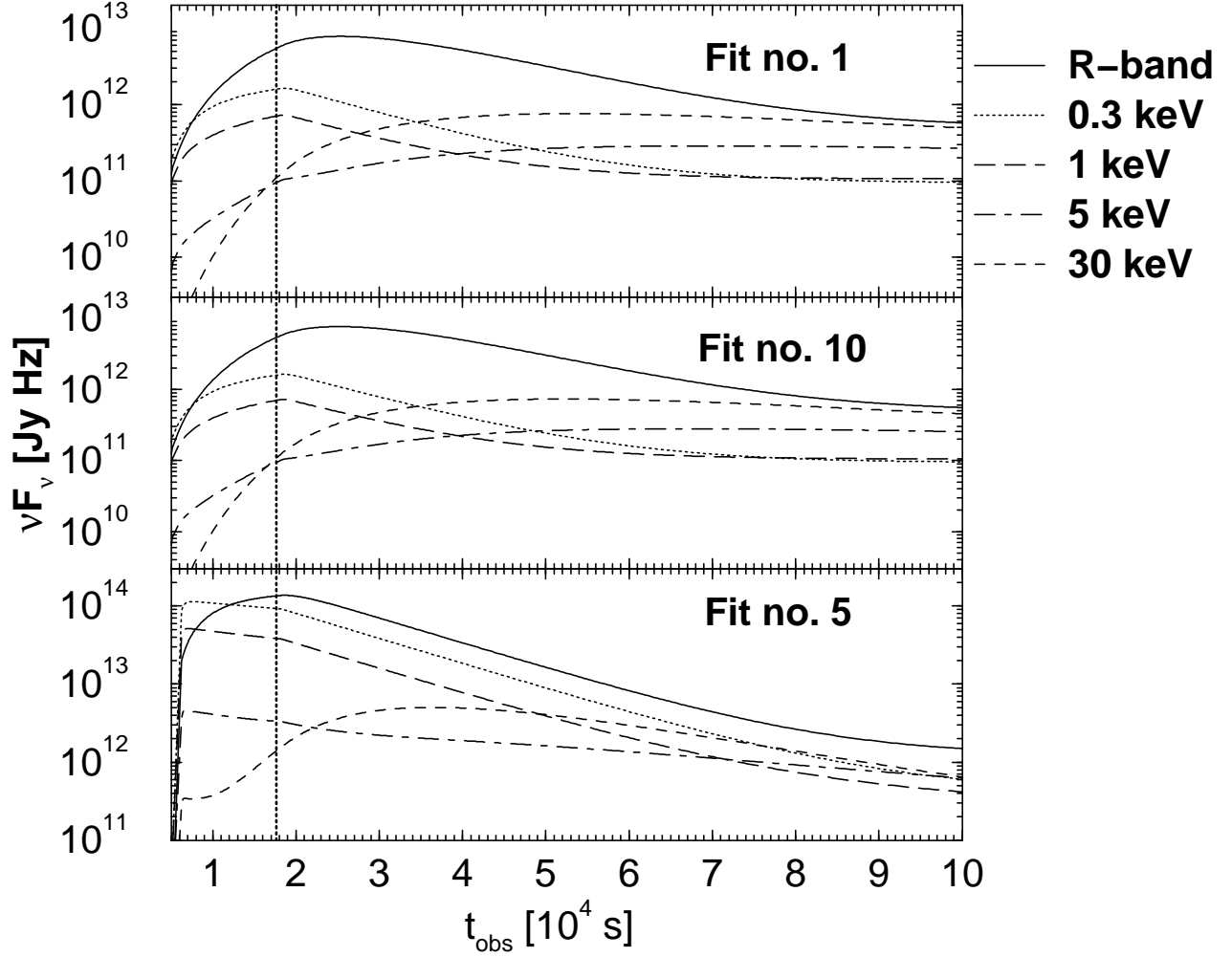


Fig. 6.— Light curves in the R-band and at 5 different X-ray energies resulting from the time-dependent simulations corresponding to spectral fits no. 1, 5, and 10, illustrated in Fig. 5. The dotted vertical line marks the end of the electron-injection flare (see text for discussion). While the SSC dominated model no. 5 produces drastically different light curves than the synchrotron dominated cases, there is no significant difference due to the addition of a moderate external-Compton component (fit no. 10).

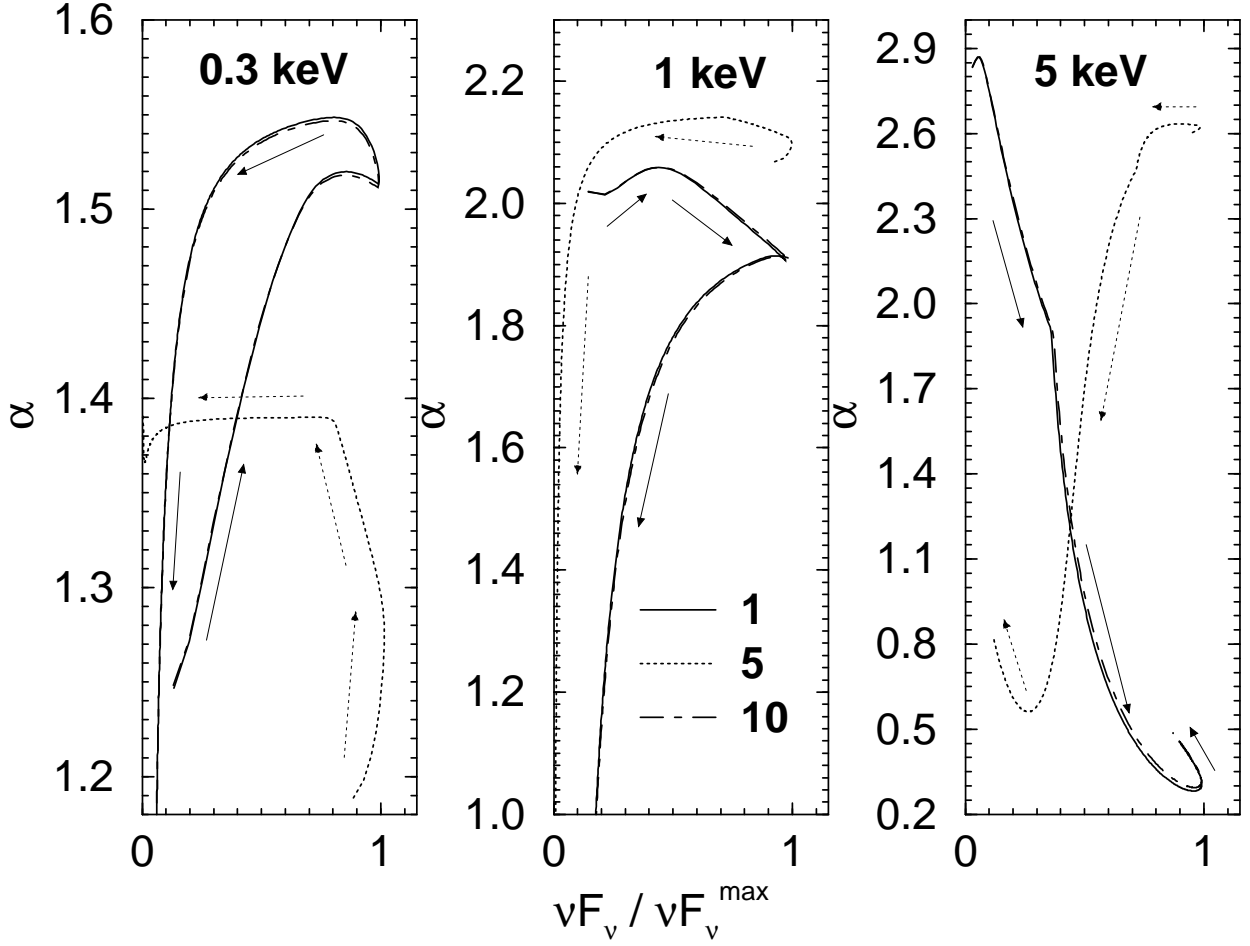


Fig. 7.— Tracks in the hardness-intensity plane resulting from the time-dependent simulations corresponding to spectral fits no. 1, 5, and 10, at 3 different X-ray energies. While the SSC dominated model no. 5 produces drastically different tracks in the hardness-intensity plane than the synchrotron dominated cases, there is no significant difference due to the addition of a moderate external-Compton component (fit no. 10).

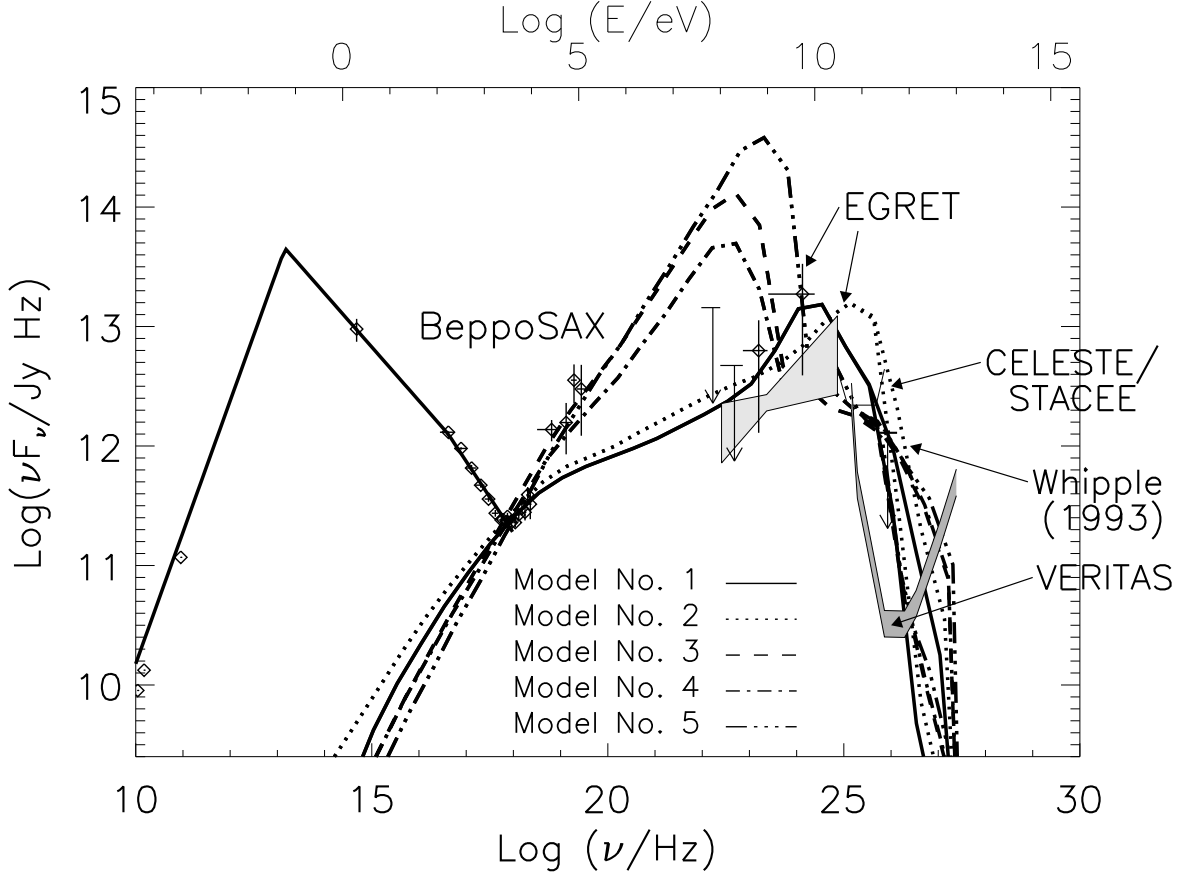


Fig. 8.— Various model fits to the SED of W Comae in March/May 1998, using the hadronic SPB model. All models are corrected for absorption in the cosmic background radiation field using the background models in Aharonian (2001). The two high-frequency branches of the model curves indicate the resulting fluxes using the two extreme background models in Aharonian (2001). The target photon field for $p - \gamma$ interactions is the primary electron synchrotron photon field, approximated by broken power laws with break energies $\epsilon_{b,1} = 0.06$ eV, $\epsilon_{b,2} = 173$ eV in the observer frame and photon spectral indices $\alpha_1 = 0.9$, $\alpha_2 = 2.45$ and $\alpha_3 = 2.6$. This target photon field is used as an input into the Monte-Carlo code to predict the high-energy component. For the complete list of model parameters, see Table 3.

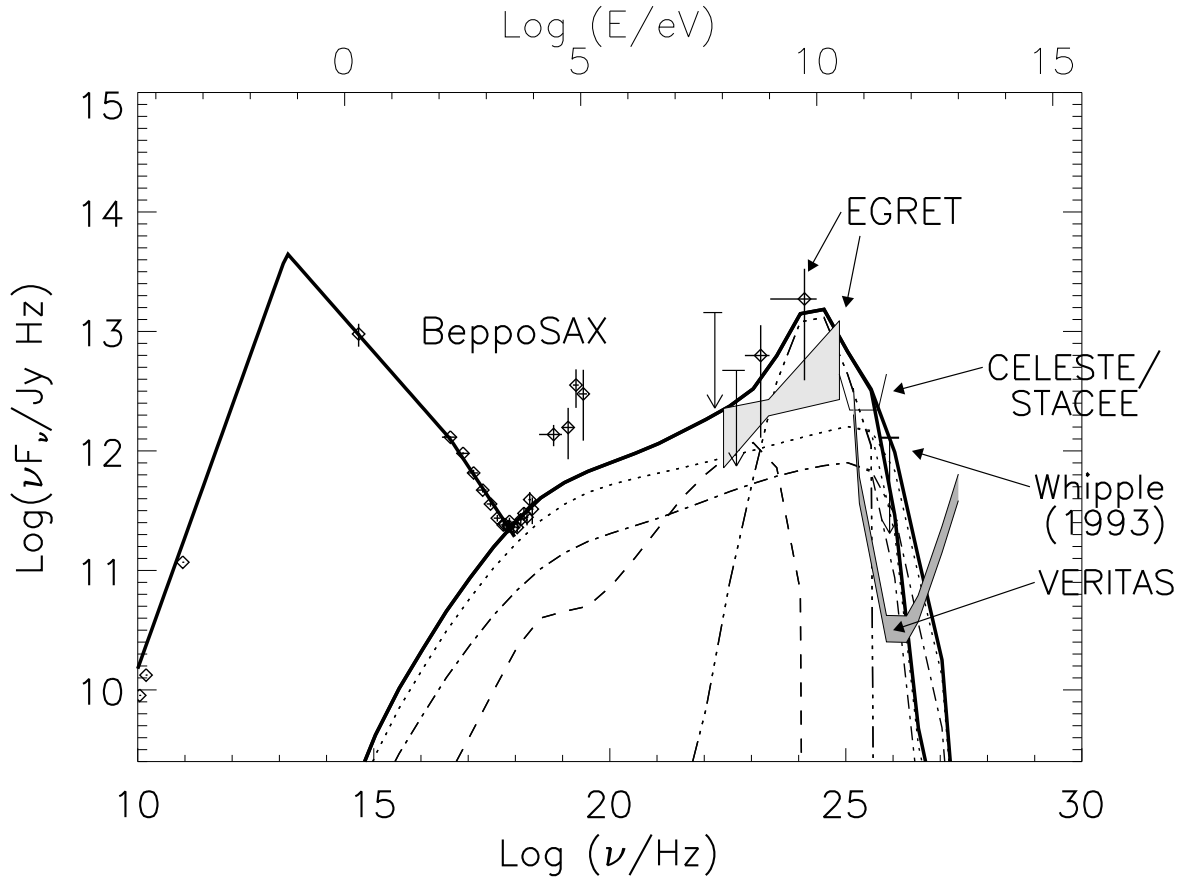


Fig. 9.— Emerging cascade spectra for SPB model 1. p synchrotron cascade (dashed line), μ synchrotron cascade (dashed-triple dot), π^0 cascade (dotted line) and π^\pm -cascade (dashed-dotted line), total (solid line). All model fluxes are corrected for absorption in the cosmic photon background as described in Fig. 8.

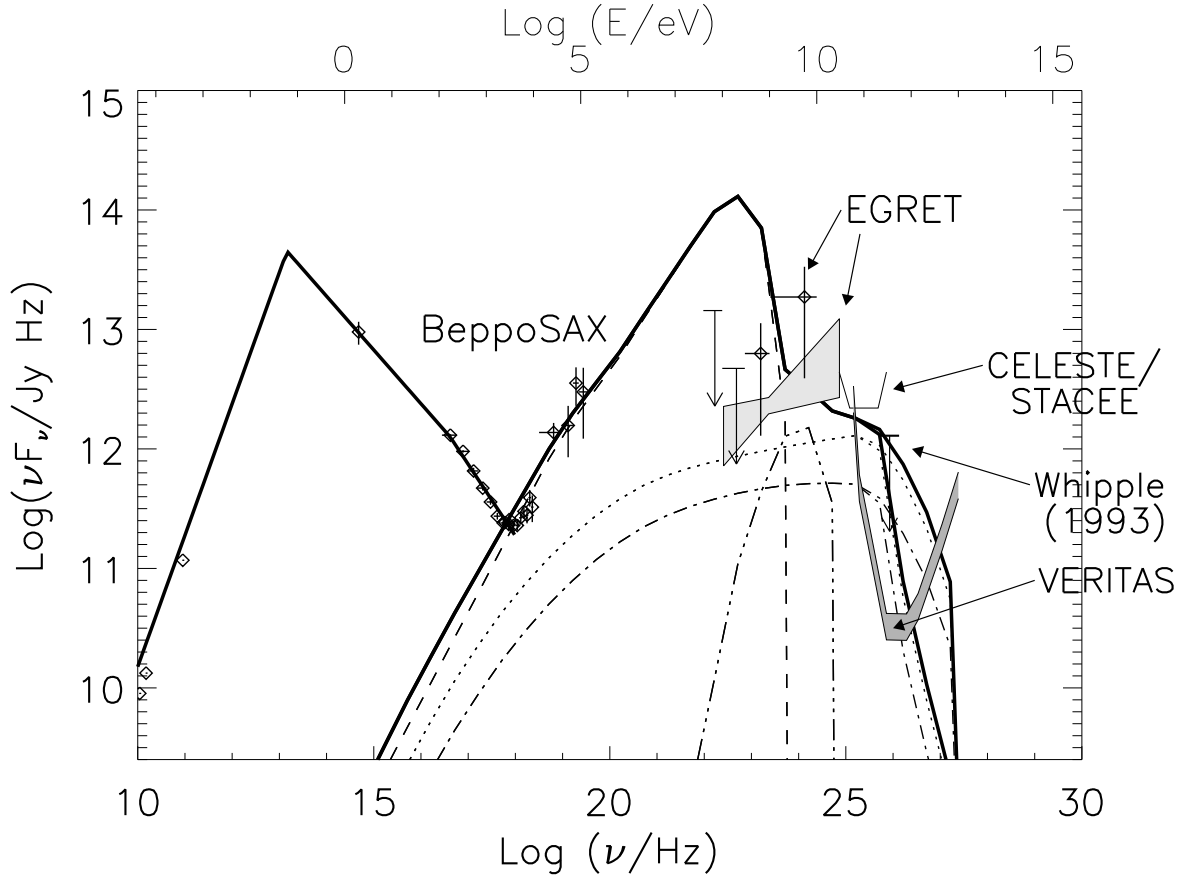


Fig. 10.— Emerging cascade spectra for SPB model 3. p synchrotron cascade (dashed line), μ synchrotron cascade (dashed-triple dot), π^0 cascade (dotted line) and π^\pm -cascade (dashed-dotted line), total (solid line). All model fluxes are corrected for absorption in the cosmic photon background as described in Fig. 8.

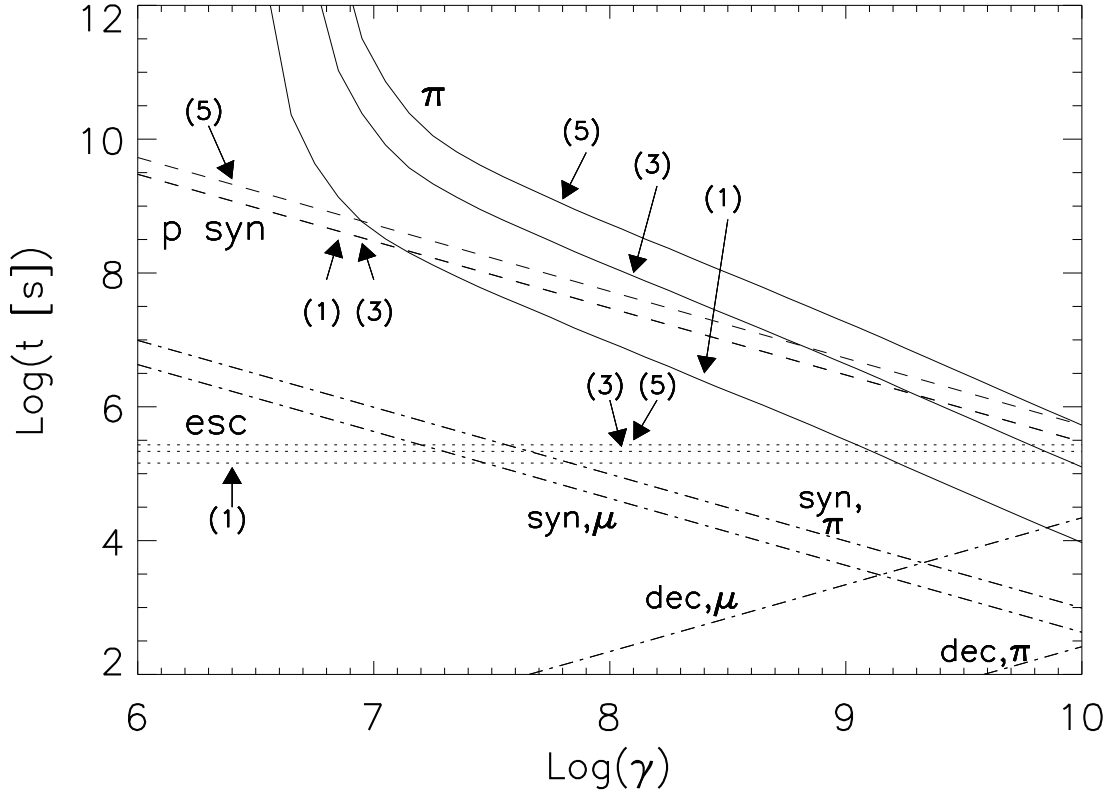


Fig. 11.— Mean energy loss times (jet frame) for the hadronic models (1), (3) and (5) for π -photoproduction (π , solid lines), p synchrotron radiation (p syn, dashed lines) and escape (dotted lines). Loss times for π^\pm and μ^\pm for synchrotron radiation (syn π , syn μ) are also shown and compared with their mean decay time scales (dec π , dec μ) for models (1) and (3).

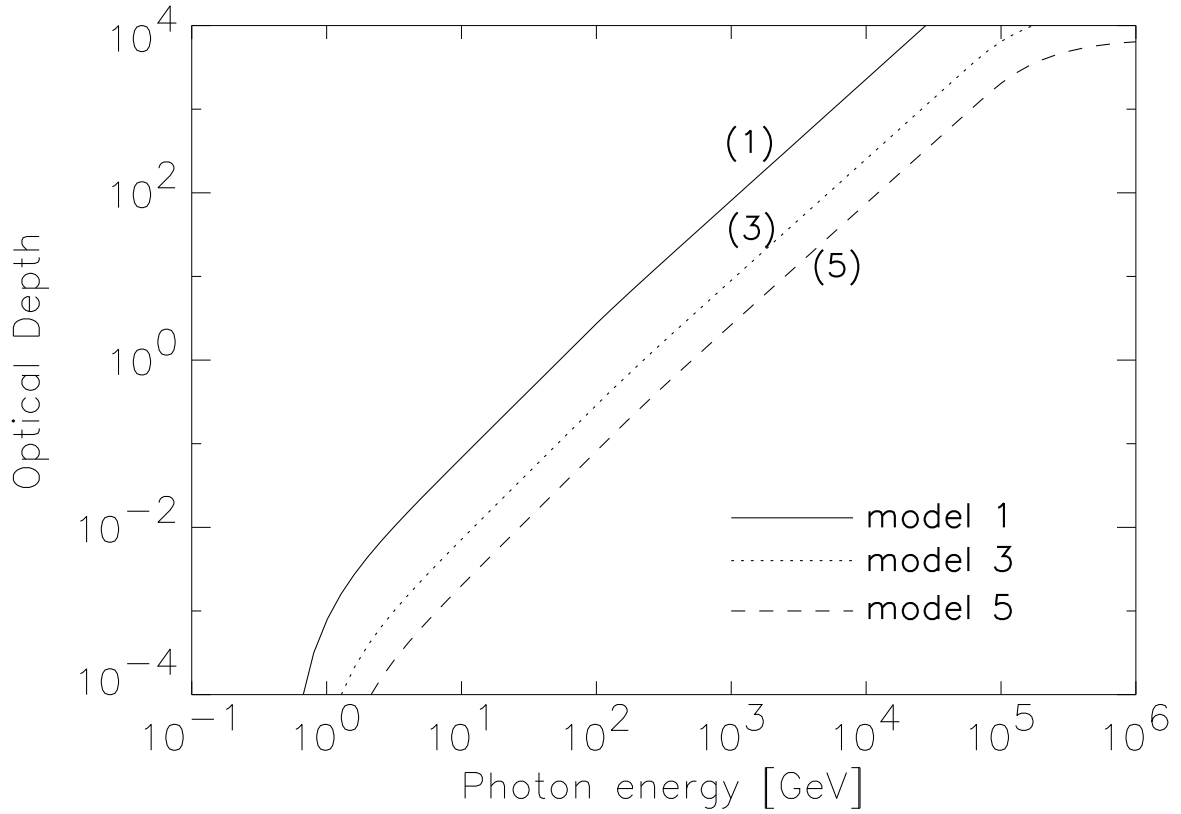


Fig. 12.— Optical depth for photon absorption in the internal (primary electron synchrotron) target photon field for the hadronic models (1), (3) and (5). Photon energies refer to the co-moving frame of the jet.

Table 1. Log of EGRET observations of W Comae. The flux in column 4 is the > 100 MeV flux in units of 10^{-8} photons $\text{cm}^{-2} \text{s}^{-1}$; the spectral index α is the photon index. Upper limits are at the 2σ level.

VP	Start date	End date	Flux	signif. [σ]	α
0020	05/30/91	06/08/91	36.4 ± 13.2	2.9	
0030	06/15/91	06/28/91	< 20.2	0.0	
0040	06/28/91	07/12/91	10.8 ± 3.9	3.5	
0110	10/03/91	10/17/91	< 25.0	0.0	
204+	12/22/92	01/12/93	23.4 ± 10.7	2.8	
2180	04/20/93	05/05/93	13.7 ± 6.9	2.5	
2220	05/24/93	05/31/93	< 35.0	0.2	
304+	10/19/93	10/25/93	15.4 ± 4.7	4.2	
3086	11/23/93	12/01/93	28.1 ± 9.4	4.3	2.02 ± 0.47
311+	12/13/93	12/20/93	17.4 ± 6.9	3.1	
3130	12/27/93	01/03/94	30.9 ± 12.7	3.1	
3220	04/05/94	04/19/94	12.2 ± 7.0	2.2	
3260	05/10/94	05/17/94	32.0 ± 13.0	3.6	
4060	12/13/94	12/20/94	< 56.4	0.2	
4180	04/25/95	05/09/95	53.6 ± 14.1	5.3	1.88 ± 0.29
5150	02/20/96	03/05/96	19.2 ± 7.1	3.3	2.54 ± 0.56
7155	03/20/98	03/27/98	38.2 ± 19.3	2.7	1.27 ± 0.58
9111	02/23/00	03/01/00	< 107.2	0.0	

Table 2. Parameters of the various fits shown in Figs. 3 and 4. $\gamma_{1,2}$, and p are the low- and high-energy cutoffs and the spectral index of the electron injection spectrum, D is the Doppler factor, $\tau_{\text{T,BLR}}$ is the radial Thomson depth of the BLR. The magnetic field B is the equipartition value.

Fit no.	γ_1	γ_2	p	n_e [cm^{-3}]	B [G]	D	$\tau_{\text{T,BLR}}$	$F(> 40 \text{ GeV})$ [$\text{ph cm}^{-2} \text{s}^{-1}$]
1	500	8.0×10^4	2.7	25	0.78	19.41	0	3.71×10^{-11}
2	700	7.5×10^4	2.6	30	1.04	19.41	0	8.33×10^{-11}
3	1000	6.2×10^4	2.5	35	1.37	19.41	0	1.62×10^{-10}
4	1300	5.3×10^4	2.3	45	1.88	19.41	0	3.25×10^{-10}
5	1600	4.8×10^4	2.2	55	2.33	19.41	0	4.45×10^{-10}
6	1000	9.0×10^4	2.4	18	1.04	7.78	0	8.59×10^{-11}
7	1000	4.0×10^4	2.2	65	2.43	28.05	0	6.83×10^{-10}
8	500	8.0×10^4	2.7	25	0.78	19.41	1×10^{-3}	4.66×10^{-11}
9	500	8.0×10^4	2.7	25	0.78	19.41	3×10^{-3}	8.32×10^{-11}
10	500	8.0×10^4	2.7	25	0.78	19.41	1×10^{-2}	1.11×10^{-10}

Table 3. Parameters of the various fits shown in Figs. 8. $n_p \propto \gamma_p^{-\alpha_p}$ is the injection proton spectrum in the energy range $2 \leq \gamma_p \leq \gamma_{p,\max}$, u_p is the injected proton energy density, e/p the injected relativistic primary electron-to-proton number ratio, D is the Doppler factor, R_b the size of the emission region and B the magnetic field. All parameters are measured in the jet frame. The predicted integrated photon fluxes above 40 GeV and 1 TeV, $F(> 40\text{GeV})$ and $F(> 1\text{TeV})$, are corrected for photon absorption in the cosmic background radiation field using the different background models in Aharonian (2001).

Fit no.	α_p	$\gamma_{p,\max}$	u_p [erg cm ⁻³]	e/p	D	R_b [10 ¹⁵ cm]	B [G]	$F(> 40 \text{ GeV})$ [ph cm ⁻² s ⁻¹]	$F(> 1 \text{ TeV})$ [ph cm ⁻² s ⁻¹]
1	1.5	1×10^9	240	1.6	8	4.3	40	$(4.5 - 6.2) \times 10^{-10}$	$(0.7 - 11) \times 10^{-14}$
2	2.0	3×10^9	300	0.2	10	5.4	40	$(8.3 - 13) \times 10^{-10}$	$(1.5 - 8.9) \times 10^{-14}$
3	1.5	5×10^8	150	0.1	12	6.5	40	$(0.8 - 1.3) \times 10^{-10}$	$(2.6 - 5.4) \times 10^{-14}$
4	1.5	5×10^8	150	0.1	12	6.5	30	$(0.9 - 1.4) \times 10^{-10}$	$(2.8 - 5.9) \times 10^{-14}$
5	1.5	1×10^9	60	0.1	15	8.1	30	$(0.7 - 1.0) \times 10^{-10}$	$(1.8 - 48) \times 10^{-14}$